Scientific Annals of Computer Science vol. 35 (1), 2025, pp. 53–85
doi: 10.47743/SACS.2025.1.53

Degree-based Topological Characterization and Graph Energy Prediction of Silicon Carbide Network Si_2C_3-$I[k,l]$ via Double Graph Operator

Vijaya Chandra Kumar U.[1], Nagesh H.M.[2], and Madhusudana Reddy M.B.[3]

Abstract

This study presents the precise formulation of the Nirmala index and the first and second inverse Nirmala indices for the double graph of the silicon carbide network Si_2C_3-I$[k,l]$, using its M-polynomial. Entropy measures based on these indices are derived using Shannon's entropy model. Numerical and graphical comparisons are conducted between the Nirmala indices and their corresponding entropy measures. Curve fitting and Pearson correlation analysis are used to examine their relationships. Finally, the computed indices are employed to develop a predictive model for the graph energy of Si_2C_3-I$[k,l]$ and estimate the HOMO-LUMO gap.

Keywords: Nirmala index, first and second inverse Nirmala index, graph entropy, silicon carbide network, double graph.

1 Introduction

Consider the ordered pair $\digamma = (V(\digamma), E(\digamma))$, which represents a simple, connected, and undirected graph characterized by a non-empty vertex set

This work is licensed under the Creative Commons Attribution Licence (CC BY)

[1]Department of Mathematics, School of Applied Sciences, REVA University, Bengaluru, India. Email: uvijaychandra.kumar@reva.edu.in

[2]Department of Science & Humanities, PES University, Bengaluru, India. Email: nageshhm@pes.edu

[3]Department of Chemistry, School of Applied Sciences, REVA University, Bengaluru, India. Email: madhusudana.mb@reva.edu.in

$V(F)$ and edge set $E(F)$. The total number of edges incident to a vertex $v \in V(F)$ is the *degree* of v and is denoted by $d_F(v)$. For any edge $e \in E(F)$, we represent it as $e = pq$, where p and q are the end vertices of e. The field of chemical graph theory applies graph theory to study and model the structural features of chemical compounds. In this approach, chemical compounds are depicted as graphs, where atoms serve as vertices and chemical bonds as edges. The mathematical analysis of molecular structures involves the use of theoretical, computational, and graphical techniques [44]. These molecular graphs include topological indices, which are mathematical measures used to predict the physical, chemical, and biological properties of compounds. Such indices are particularly useful in research related to Quantitative Structure-Property Relationships (QSPR) and Quantitative Structure-Activity Relationships (QSAR) [1, 24, 25, 48].

As given in [10], the degree-based topological index, which is defined on the edge set $E(F)$ of a graph F is expressed as follows:

$$I(F) = \sum_{uv \in E(F)} f(d_F(u), d_F(v)),$$

where $f(x, y)$ is a non-negative and symmetric function that depends on the mathematical formulation of the topological index.

Topological indices have been extensively studied in the literature and have demonstrated their utility across various fields, including drug discovery, chemistry, biology, computer science, and mathematics. The Wiener index, introduced by H. Wiener in 1947, was the first topological index and remains one of the most widely investigated. It has been particularly effective in predicting the boiling points of paraffin compounds [47]. Another prominent degree-based measure is the Randić index, also known as the connectivity index, which was proposed by Milan Randić in 1975 and has found significant applications in drug discovery [35]. For a comprehensive overview of topological indices and their diverse applications, readers may refer to [13, 14].

To enhance the predictive capabilities of existing topological indices, several new degree-based indices have been developed. In [19], Kulli introduced a new degree-based topological index for a molecular graph F, known as the *Nirmala index*, which is defined as follows:

$$N(F) = \sum_{uv \in E(F)} \sqrt{d_F(u) + d_F(v)}. \tag{1}$$

In 2021, Kulli [20] further introduced the concepts of the first inverse Nirmala index $IN_1(F)$ and the second inverse Nirmala index $IN_2(F)$ for a molecular graph G, defined as follows:

$$IN_1(F) = \sum_{uv \in E(F)} \sqrt{\frac{1}{d_F(u)} + \frac{1}{d_F(v)}} = \sum_{uv \in E(F)} \left(\frac{1}{d_F(u)} + \frac{1}{d_F(v)}\right)^{\frac{1}{2}}, \quad (2)$$

$$IN_2(F) = \sum_{uv \in E(F)} \frac{1}{\sqrt{\frac{1}{d_F(u)} + \frac{1}{d_F(v)}}} = \sum_{uv \in E(F)} \left(\frac{1}{d_F(u)} + \frac{1}{d_F(v)}\right)^{-\frac{1}{2}}. \quad (3)$$

Historically, numerous topological indices have been calculated using traditional mathematical formulations. There have been various efforts to explore a more compact approach that can retrieve multiple topological indices belonging to a specific category. In this context, the notion of a general polynomial was presented, which uses its derivatives, integrals, or a combination of these operations to provide the necessary values of topological indices at a given place. For example, the Hosoya polynomial is used to recover distance-based topological indices [15], while the NM-polynomial is responsible for generating topological indices based on the neighborhood degree sum [45]. The concept of the M-polynomial was introduced by Deutsch and Klažar in [11], aimed at determining degree-based topological indices.

Definition 1. *The M-polynomial of a graph F is defined as follows:*

$$M(F;x,y) = \sum_{\delta \le i \le j \le \Delta} m_{i,j}(F) x^i y^j,$$

where $\delta = min\{d_F(u)|u \in V(F)\}$, $\Delta = max\{d_F(u)|u \in V(F)\}$, and $m_{i,j}(F)$ is the number of edges $uv \in E(F)$ such that $d_F(u) = i, d_F(v) = j\ (i,j \ge 1)$.

The derivation formulas for various Nirmala indices based on the M-polynomial are presented in Table 1.

Sl. No	Topological Index	$f(x,y)$	Derivation from $M(\digamma;x,y)$
1	Nirmala index (N)	$\sqrt{x+y}$	$D_x^{\frac{1}{2}}J(M(\digamma;x,y))\|_{x=1}$
2	First inverse Nirmala index (IN_1)	$\sqrt{\frac{x+y}{xy}}$	$D_x^{\frac{1}{2}}JS_y^{\frac{1}{2}}S_x^{\frac{1}{2}}(M(\digamma;x,y))\|_{x=1}$
3	Second inverse Nirmala index (IN_2)	$\sqrt{\frac{xy}{x+y}}$	$S_x^{\frac{1}{2}}JD_y^{\frac{1}{2}}D_x^{\frac{1}{2}}(M(\digamma;x,y))\|_{x=1}$

Table 1: Relation between the Nirmala indices and the M-polynomial of a graph $\digamma$.

Here, $D_x^{\frac{1}{2}}(h(x,y)) = \sqrt{x\cdot\frac{\partial(h(x,y))}{\partial x}}\cdot\sqrt{h(x,y)}$;
$D_y^{\frac{1}{2}}(h(x,y)) = \sqrt{y\cdot\frac{\partial(h(x,y))}{\partial y}}\cdot\sqrt{h(x,y)}$;
$S_x^{\frac{1}{2}}(h(x,y)) = \sqrt{\int_0^x \frac{h(t,y)}{t}dt}\cdot\sqrt{h(x,y)}$;
$S_y^{\frac{1}{2}}(h(x,y)) = \sqrt{\int_0^y \frac{h(x,t)}{t}dt}\cdot\sqrt{h(x,y)}$; and $J(h(x,y)) = h(x,x)$ are the operators.

For further information on degree-based topological indices derived using the M-polynomial, readers are referred to [3,4,7–9,17,26,27,30,32,34,41–43].

Using probability distributions, Shannon [38] first proposed the idea of entropy to measure the degree of information uncertainty in a system. Later, this idea was expanded to include the analysis of chemical structures, networks, and graphs' structural information. In a number of disciplines, including computer science, biology, chemistry, sociology, ecology, and mathematics, graph entropy has become increasingly important in recent years. The probability distributions of graph invariants, such as vertices and edges, are linked to several kinds of graph entropy metrics, including extrinsic and intrinsic measures. See [16,22,23,28,29,31,33,39,40,46] for additional information on degree-based graph entropy measurements and their uses.

1.1 Entropy of a Graph in Terms of Edge-Weight

Chen et al. [2] introduced the notion of entropy in the context of edge-weighted graphs, detailing its foundational principles. Consider the graph $\digamma = (V(\digamma), E(\digamma), \omega(st))$, where $V(\digamma)$ represents the set of vertices, $E(\digamma)$ be set of edges, and $\omega(st)$ indicates the weight associated with an edge $st \in E(\digamma)$. The entropy of $\digamma$, in relation to its edge weights, is subsequently defined as follows:

$$\begin{aligned} ENT_{\omega}(\digamma) &= -\sum_{s't' \in E(\digamma)} \frac{\omega(s't')}{\sum_{st \in E(\digamma)} \omega(st)} log\left(\frac{\omega(s't')}{\sum_{st \in E(\digamma)} \omega(st)}\right) \\ &= -\sum_{s't' \in E(\digamma)} \frac{\omega(s't')}{\sum_{st \in E(\digamma)} \omega(st)} \left[log(\omega(s't')) - log\left(\sum_{st \in E(\digamma)} \omega(st)\right)\right] \\ &= log\left(\sum_{st \in E(\digamma)} \omega(st)\right) - \sum_{s't' \in E(\digamma)} \frac{\omega(s't')}{\sum_{st \in E(\digamma)} \omega(st)} log(\omega(s't')). \end{aligned}$$

Hence,

$$\begin{aligned} ENT_{\omega}(\digamma) = & \ log\left(\sum_{st \in E(\digamma)} \omega(st)\right) \\ & - \frac{1}{\left(\sum_{st \in E(\digamma)} \omega(st)\right)} \sum_{s't' \in E(\digamma)} \omega(s't') log(\omega(s't')). \end{aligned} \tag{4}$$

Virendra Kumar et al. [21] introduced the idea of entropy based on Nirmala indices in a recent study. As shown in (1)-(3), they defined the relevant information function ω in terms of the Nirmala indices.

Nirmala entropy: Define $\omega(st) = \sqrt{d_{\digamma}(s) + d_{\digamma}(t)}$. Consequently, based on the definition of the Nirmala index presented in (1), we obtain,

$$\sum_{st \in E(\digamma)} \omega(st) = \sum_{st \in E(\digamma)} \sqrt{d_{\digamma}(s) + d_{\digamma}(t)} = N(\digamma).$$

Thus, by using (4), the Nirmala entropy of a graph F is expressed as:

$$ENT_N(F) = log(N(F)) - \frac{1}{N(F)} \sum_{st \in E(F)} \sqrt{d_F(s) + d_F(t)} \times log(\sqrt{d_F(s) + d_F(t)}). \quad (5)$$

First inverse Nirmala entropy: Define $\omega(st) = \sqrt{\frac{1}{d_F(s)} + \frac{1}{d_F(t)}}$. Based on the definition established for the first inverse Nirmala index in (2), it can be deduced that

$$\sum_{st \in E(F)} \omega(st) = \sum_{st \in E(F)} \sqrt{\frac{1}{d_F(s)} + \frac{1}{d_F(t)}} = IN_1(F).$$

Thus, by using (4), the first inverse Nirmala entropy of a graph F is expressed as:

$$ENT_{IN_1}(F) = log(IN_1(F)) - \frac{1}{IN_1(F)} \sum_{st \in E(F)} \sqrt{\frac{1}{d_F(s)} + \frac{1}{d_F(t)}} \times log\left(\sqrt{\frac{1}{d_F(s)} + \frac{1}{d_F(t)}}\right). \quad (6)$$

Second inverse Nirmala entropy: Define the function $\omega(st)$ as follows: $\omega(st) = \frac{\sqrt{d_F(s) \cdot d_F(t)}}{\sqrt{d_F(s) + d_F(t)}}$. Consequently, based on the definition of the second inverse Nirmala index presented in (3), we can derive the following.

$$\sum_{st \in E(F)} \omega(st) = \sum_{st \in E(F)} \frac{\sqrt{d_F(s) \cdot d_F(t)}}{\sqrt{d_F(s) + d_F(t)}} = IN_2(F).$$

Hence, using (4), the second inverse Nirmala entropy of a graph F is given by

$$ENT_{IN_2}(F) = log(IN_2(F)) - \frac{1}{IN_2(F)} \sum_{st \in E(F)} \frac{\sqrt{d_F(s) \cdot d_F(t)}}{\sqrt{d_F(s) + d_F(t)}} \times log\left(\frac{\sqrt{d_F(s) \cdot d_F(t)}}{\sqrt{d_F(s) + d_F(t)}}\right). \quad (7)$$

2 Silicon Carbide Si_2C_3-$I[k,l]$ 2D Structure and Its Double Graph

Silicon carbide is a semiconductor material that is well-suited to high-temperature electrical and electro-optical applications. Silicon carbide, a critical non-oxide ceramic, is widely used in manufacturing due to its unique qualities, which include remarkable stiffness and strength, thermal and chemical stability, a high melting point, oxidation resistance, and great erosion resistance. Because of these characteristics, silicon carbide is the optimal material for high-power, high-temperature electrical devices, as well as for erosion and cutting applications. Due to the various applications of silicon carbide, topological and entropy properties also emerge as important tools for development.

The silicon carbide Si_2C_3-$I[k,l]$ represents a two-dimensional molecular graph, as depicted in Figure 1. To describe this molecular graph, the following parameters are considered: the parameter k represents the number of interconnected unit cells arranged in a linear sequence (chain), as shown in Figure 1(a), while l denotes the number of interconnected rows, where each row consists of k cells. Figure 1(b) illustrates the interconnections between the cells within a single row (chain) as well as the relationships among different rows. Furthermore, Figure 1(c) shows the structure of a one-dimensional unit cell.

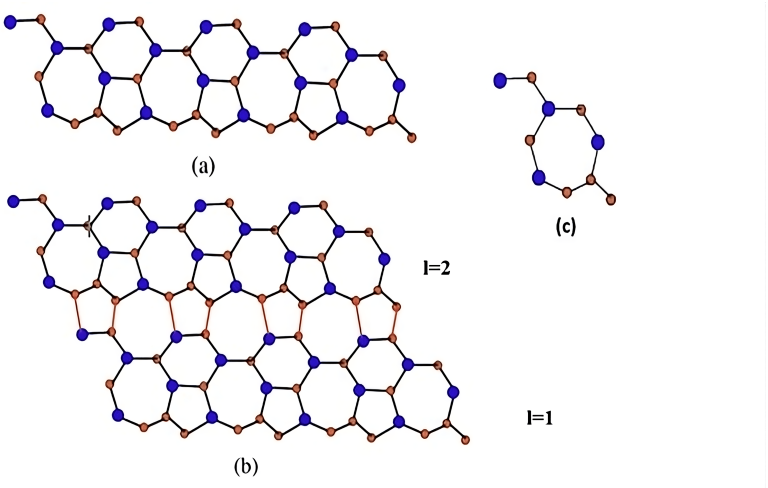

Figure 1: Two-dimensional structure of Si_2C_3-$I[k,l]$.

2.1 Double Graph of Silicon Carbide Network of $Si_2C_3 - I[k,l]$

The *double graph* of a graph G is obtained by creating two identical copies of G (including their respective edge sets) and introducing edges u_1v_2 and v_1u_2 for each edge uv in G.

Let $D(Si_2C_3\text{-I}[k,l])$ denote the double graph of the silicon carbide Si_2C_3-$I[k,l]$. The construction of $D(Si_2C_3\text{-I}[k,l])$ is as follows: Take two copies of the graph Si_2C_3-$I[k,l]$, say C_1 and C_2, where $(k,l \geq 1)$. Connect each vertex in C_1 to its corresponding neighbor in C_2. The double graph of the silicon carbide network Si_2C_3-$I[1,1]$ [37] being analyzed is depicted in Figure 2.

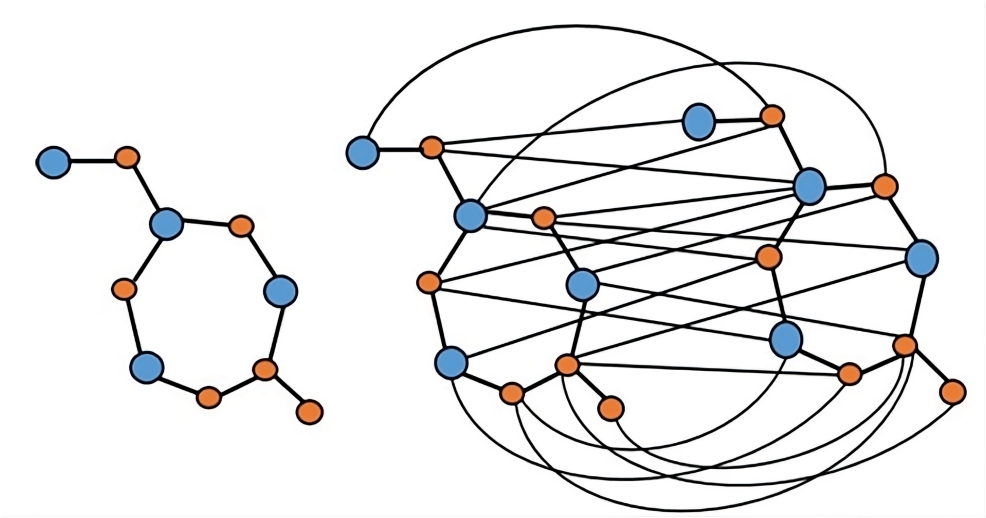

Figure 2: Silicon carbide Si_2C_3-$I[1,1]$ and $D(Si_2C_3$-$I[1,1])$.

2.2 Novelty and Motivation

There are many graph operators with which one can construct a new graph from a given graph, such as line graphs, double graphs, total graphs, middle graphs, and their generalizations.

Topological indices of graph operators are essential as they offer valuable insights into the structural and chemical characteristics of the graphs they represent [18]. Few research have used graph operators to investigate the topological and entropy-based characteristics of silicon carbide networks in recent years [5, 6]. Sardar et al. in [37] investigated certain degree-based topological indices of the double graph of the silicon carbide network Si_2C_3-I$[k,l]$. Similarly, Khan et al. in [18] focused on the entropy measures of the double and strong double graph of the same network and performed QSPR analysis for four mechanical characteristics such as, Poisson's ratio, shear modulus, Young's modulus, and bulk modulus using linear and quadratic regression models. Although these studies establish a solid foundation for understanding the structural properties and behavior of silicon carbide networks, there remains a need for further investigation to reveal more profound insights into the relationship between topological indices and their associated entropy measures. Such an investigation could provide a more comprehensive understanding of the networks stability and functionality.

Given the wide range of applications of silicon carbide, both topological and entropy properties have become crucial tools for its development. Nirmala indices, particularly the first inverse Nirmala index, exhibit unusual behavior compared to other indices and possess significant predictive potential [12]. As far as we know, no research has been conducted on Nirmala-based indices of graph operators applied to silicon carbide networks. This study focuses on computing the Nirmala index, as well as the first and second inverse Nirmala indices, for the double graph of the silicon carbide network Si_2C_3-$I[k,l]$. The HOMO-LUMO gap is found for particular dimensions of Si_2C_3-$I[k,l]$, and a predictive model for the graph energy of the silicon carbide network Si_2C_3-$I[k,l]$ are developed using the calculated indices values of the double graph.

2.3 Methodology

In this paper, we investigate the structural properties of the double graph of the silicon carbide network Si_2C_3-$I[k,l]$. Shannon's entropy measures are applied using novel information functions derived from various definitions of the Nirmala index. A comprehensive mathematical and computational analysis of these measures is carried out for the double graph of Si_2C_3-$I[k,l]$.

The paper is organized as follows: Section 2 explores the two-dimensional structure of Si_2C_3-$I[k,l]$ and its corresponding double graph. Section 3 focuses on the computation of the Nirmala indices for the double graph of

Si_2C_3-$I[k,l]$ using its M-polynomial, along with the evaluation of entropy measures based on these indices. Section 4 provides a comparison of the Nirmala indices and their respective entropy measures through numerical data and graphical visualizations for the double graph of Si_2C_3-$I[k,l]$, where $1 \leq k,l \leq 100$ and $k = l$. In Section 5, we construct optimal regression models to establish relationships between the Nirmala indices and the corresponding entropies using MATLAB R2019a's curve-fitting tool. Section 6 employs Python to compute the Pearson correlation between the Nirmala indices and their associated entropy measures for the double graph of Si_2C_3-$I[k,l]$, where $1 \leq k,l \leq 100$ and $k = l$. Section 7 examines the HOMO-LUMO gap and develops a predictive model for the graph energy of the silicon carbide network Si_2C_3-$I[k,l]$. Finally, Sections 8 and 9 present the discussion and conclusion, respectively.

3 Main Results

The double graph of the silicon carbide network Si_2C_3-$I[k,l]$ has been thoroughly examined in [18,37], where a number of degree-based topological indices were calculated using the vertex-degree-based edge set partition technique. The Nirmala index, the first and second inverse Nirmala indices, and the associated graph entropies will now be computed. $D(Si_2C_3$-$I[k,l])$ has the order $20kl$ and the size $60kl - 8k - 12l$. Table 2 provides the edge set partition of $D(Si_2C_3$-$I[k,l])$.

Sl. No	Edge set	$(d_F(r), d_F(s))$	Number of repetitions
1	E_1	(2,4)	4
2	E_2	(2,6)	4
3	E_3	(4,4)	$4k + 8l$
4	E_4	(4,6)	$24k + 32l - 36$
5	E_5	(6,6)	$60kl - 36k - 52l + 28$

Table 2: The edge set partitions of $D(Si_2C_3$-$I[k,l])$.

3.1 Nirmala Indices of $D(Si_2C_3$-$I[k,l])$

In this section, we first find the M-polynomial of $D(Si_2C_3$-$I[k,l])$.

Theorem 1. *Let $\digamma$ be the double graph of silicon carbide network Si_2C_3-$I[k,l]$. Then the M-polynomial of $\digamma$ is*
$M(\digamma;x,y) = 4x^2y^4 + 4x^2y^6 + (4k+8l)x^4y^4 + (24k+32l-36)x^4y^6 + (60kl - 36k - 52l + 28)x^6y^6$.

Proof. Let $\digamma$ be the double graph of silicon carbide network Si_2C_3-$I[k,l]$. Since each vertex of $\digamma$ is of degree either 2 or 4 or 6, the partitions of edge set $E(\digamma)$ are:

$E_1(\digamma) := \{e = ab \in E(\digamma) : d_\digamma(a) = 2, d_\digamma(b) = 4\}$;
$E_2(\digamma)) := \{e = ab \in E(\digamma) : d_\digamma(a) = 2, d_\digamma(b) = 6\}$;
$E_3(\digamma) := \{e = ab \in E(\digamma) : d_\digamma(a) = 4, d_\digamma(b) = 4\}$;
$E_4(\digamma) := \{e = ab \in E(\digamma) : d_\digamma(a) = 4, d_\digamma(b) = 6\}$.
$E_5(\digamma) := \{e = ab \in E(\digamma) : d_\digamma(a) = 6, d_\digamma(b) = 6\}$.

Clearly, $|E_1(\digamma)| = 4; |E_2(\digamma)| = 4; |E_3(\digamma)| = 4k + 8l; |E_4(\digamma)| = 24k + 32l - 36; |E_5(\digamma)| = 60kl - 36k - 52l + 28$. Therefore,

$$M(\digamma;x,y) = 4x^2y^4 + 4x^2y^6 + (4k+8l)x^4y^4 + (24k+32l-36)x^4y^6 + (60kl - 36k - 52l + 28)x^6y^6.$$ □

We now evaluate the Nirmala indices of $D(Si_2C_3$-$I[k,l])$ using its M-polynomial.

Theorem 2. *Let $\digamma$ be the double graph of silicon carbide Si_2C_3-$I[k,l]$. Then*

$$\begin{aligned}
N(\digamma) =& (4\sqrt{6} + 4\sqrt{8} + 28\sqrt{12} - 36\sqrt{10}) + k\left(4\sqrt{8} + 24\sqrt{10} - 36\sqrt{12}\right) \\
&+ l\left(8\sqrt{8} + 32\sqrt{10} - 52\sqrt{12}\right) + 60\left(kl\sqrt{12}\right), \\
IN_1(\digamma) =& \left(2\sqrt{3} + \frac{8}{\sqrt{6}} + \frac{28}{\sqrt{3}} - 36\sqrt{\frac{10}{24}}\right) + k\left(\frac{4}{\sqrt{2}} + 24\sqrt{\frac{10}{24}} - \frac{36}{\sqrt{3}}\right) \\
&+ l\left(\frac{8}{\sqrt{2}} + 32\sqrt{\frac{10}{24}} - \frac{52}{\sqrt{3}}\right) + 60\left(\frac{kl}{\sqrt{3}}\right), \\
IN_2(\digamma) =& \left(8\sqrt{3} + 2\sqrt{6} + 28\sqrt{3} - 36\sqrt{\frac{24}{10}}\right) + k\left(4\sqrt{2} + 24\sqrt{\frac{24}{10}} - 36\sqrt{3}\right) \\
&+ l\left(8\sqrt{2} + 32\sqrt{\frac{24}{10}} - 52\sqrt{3}\right) + 60\left(kl\sqrt{3}\right).
\end{aligned}$$

Proof. Let $\digamma$ be the double graph of silicon carbide Si_2C_3-$I[k,l]$. Then the M-polynomial of $\digamma$ is

$$M(\digamma;x,y) = 4x^2y^4 + 4x^2y^6 + (4k+8l)x^4y^4 + (24k+32l-36)x^4y^6 + (60kl-36k-52l+28)x^6y^6.$$

From Table 1, we have

$$\begin{aligned}
&(i)\, D_x^{\frac{1}{2}} J(M(\digamma;x,y)) \\
&= D_x^{\frac{1}{2}} J \left[\begin{array}{l} 4x^2y^4 + 4x^2y^6 + (4k+8l)x^4y^4 + (24k+32l-36)x^4y^6 \\ +(60kl-36k-52l+28)x^6y^6 \end{array} \right] \\
&= D_x^{\frac{1}{2}} \left[\begin{array}{l} 4x^6 + 4x^8 + (4k+8l)x^8 + (24k+32l-36)x^{10} \\ +(60kl-36k-52l+28)x^{12} \end{array} \right] \\
&= 4\sqrt{6}x^6 + 4\sqrt{8}x^8 + \sqrt{8}(4k+8l)x^8 + \sqrt{10}(24k+32l-36)x^{10} \\
&\quad + \sqrt{12}(60kl-36k-52l+28)x^{12} \\
&= 4\sqrt{6}x^6 + \sqrt{8}(4k+8l+4)x^8 + \sqrt{10}(24k+32l-36)x^{10} \\
&\quad + \sqrt{12}(60kl-36k-52l+28)x^{12},
\end{aligned}$$

$$\begin{aligned}
&(ii)\, D_x^{\frac{1}{2}} J S_y^{\frac{1}{2}} S_x^{\frac{1}{2}} (M(\digamma;x,y)) \\
&= D_x^{\frac{1}{2}} J S_y^{\frac{1}{2}} S_x^{\frac{1}{2}} \left[4x^2y^4 + 4x^2y^6 + (4k+8l)x^4y^4 + (24k+32l-36)x^4y^6 \right] \\
&\quad + D_x^{\frac{1}{2}} J S_y^{\frac{1}{2}} S_x^{\frac{1}{2}} \left[(60kl-36k-52l+28)x^6y^6 \right] \\
&= D_x^{\frac{1}{2}} J S_y^{\frac{1}{2}} \left[2\sqrt{2}x^2y^4 + 2\sqrt{2}x^2y^6 + \frac{1}{2}(4k+8l)x^4y^4 + \frac{1}{2}(24k+32l-36)x^4y^6 \right] \\
&\quad + D_x^{\frac{1}{2}} J S_y^{\frac{1}{2}} \left[\frac{1}{\sqrt{6}}(60kl-36k-52l+28)x^6y^6 \right] \\
&= D_x^{\frac{1}{2}} J \left[\sqrt{2}x^2y^4 + \frac{2}{\sqrt{3}}x^2y^6 + \frac{1}{4}(4k+8l)x^4y^4 + \frac{1}{2\sqrt{6}}(24k+32l-36)x^4y^6 \right] \\
&\quad + D_x^{\frac{1}{2}} J \left[\frac{1}{6}(60kl-36k-52l+28)x^6y^6 \right] \\
&= D_x^{\frac{1}{2}} \left[\sqrt{2}x^6 + \frac{2}{\sqrt{3}}x^8 + \frac{1}{4}(4k+8l)x^8 + \frac{1}{2\sqrt{6}}(24k+32l-36)x^{10} \right] \\
&\quad + D_x^{\frac{1}{2}} \left[\frac{1}{6}(60kl-36k-52l+28)x^{12} \right]
\end{aligned}$$

$$=\sqrt{12}x^6+2\sqrt{\frac{8}{3}}x^8+\sqrt{8}(k+2l)x^8+\sqrt{\frac{10}{24}}(24k+32l-36)x^{10}$$
$$+\frac{(60kl-36k-52l+28)}{\sqrt{3}}x^{12},$$

$(iii)\ S_x^{\frac{1}{2}}JD_y^{\frac{1}{2}}D_x^{\frac{1}{2}}(M(F;x,y))$

$$=S_x^{\frac{1}{2}}JD_y^{\frac{1}{2}}D_x^{\frac{1}{2}}\left[4x^2y^4+4x^2y^6+(4k+8l)x^4y^4+(24k+32l-36)x^4y^6\right]$$
$$+S_x^{\frac{1}{2}}JD_y^{\frac{1}{2}}D_x^{\frac{1}{2}}\left[(60kl-36k-52l+28)x^6y^6\right]$$
$$=S_x^{\frac{1}{2}}JD_y^{\frac{1}{2}}\left[4\sqrt{2}x^2y^4+4\sqrt{2}x^2y^6+2(4k+8l)x^4y^4+2(24k+32l-36)x^4y^6\right]$$
$$+S_x^{\frac{1}{2}}JD_y^{\frac{1}{2}}\left[\sqrt{6}(60kl-36k-52l+28)x^6y^6\right]$$
$$=S_x^{\frac{1}{2}}J\left[8\sqrt{2}x^2y^4+4\sqrt{12}x^2y^6+4(4k+8l)x^4y^4+2\sqrt{6}(24k+32l-36)x^4y^6\right]$$
$$+S_x^{\frac{1}{2}}J\left[6(60kl-36k-52l+28)x^6y^6\right]$$
$$=S_x^{\frac{1}{2}}\left[8\sqrt{2}x^6+4\sqrt{12}x^8+4(4k+8l)x^8+2\sqrt{6}(24k+32l-36)x^{10}\right]$$
$$+S_x^{\frac{1}{2}}\left[6(60kl-36k-52l+28)x^{12}\right]$$
$$=\frac{8}{\sqrt{3}}x^6+\sqrt{24}x^8+\sqrt{2}(4k+8l)x^8+2\sqrt{\frac{3}{5}}(24k+32l-36)x^{10}$$
$$+\sqrt{3}(60kl-36k-52l+28)x^{12}.$$

Hence,

$$(a)\ N(F)=D_x^{\frac{1}{2}}J(M(F;x,y))|_{x=1}$$
$$=(4\sqrt{6}+4\sqrt{8}+28\sqrt{12}-36\sqrt{10})+k\left(4\sqrt{8}+24\sqrt{10}-36\sqrt{12}\right)$$
$$+l\left(8\sqrt{8}+32\sqrt{10}-52\sqrt{12}\right)+60\left(kl\sqrt{12}\right),$$

$$(b)\ IN_1(F)=D_x^{\frac{1}{2}}JS_y^{\frac{1}{2}}S_x^{\frac{1}{2}}(M(F;x,y))|_{x=1}$$
$$=(2\sqrt{3}+\frac{8}{\sqrt{6}}+\frac{28}{\sqrt{3}}-36\sqrt{\frac{10}{24}})+k\left(\frac{4}{\sqrt{2}}+24\sqrt{\frac{10}{24}}-\frac{36}{\sqrt{3}}\right)$$
$$+l\left(\frac{8}{\sqrt{2}}+32\sqrt{\frac{10}{24}}-\frac{52}{\sqrt{3}}\right)+60\left(\frac{kl}{\sqrt{3}}\right),$$

$$
\begin{aligned}
(c)\, IN_2(F) =& S_x^{\frac{1}{2}} JD_y^{\frac{1}{2}} D_x^{\frac{1}{2}} (M(F;x,y))|_{x=1} \\
=& \left(8\sqrt{3}+2\sqrt{6}+28\sqrt{3}-36\sqrt{\frac{24}{10}}\right)+k\left(4\sqrt{2}+24\sqrt{\frac{24}{10}}-36\sqrt{3}\right) \\
&+l\left(8\sqrt{2}+32\sqrt{\frac{24}{10}}-52\sqrt{3}\right)+60\left(kl\sqrt{3}\right).
\end{aligned}
$$

□

3.2 Entropy Measures of Nirmala Indices of $D(Si_2C_3$-$I[k,l])$

We continue to calculate the graph entropy measures for $D(Si_2C_3$-$I[k,l])$. Using the earlier derived formulas for the Nirmala indices, we develop the mathematical expressions for entropy measures based on these indices.

Nirmala entropy of $D(Si_2C_3$-$I[k,l])$:
The Nirmala index of F is given by

$$
\begin{aligned}
N(F) =& (4\sqrt{6}+4\sqrt{8}+28\sqrt{12}-36\sqrt{10})+k\left(4\sqrt{8}+24\sqrt{10}-36\sqrt{12}\right) \\
&+60\left(kl\sqrt{12}\right)+l\left(8\sqrt{8}+32\sqrt{10}-52\sqrt{12}\right).
\end{aligned}
$$

From (5) and Table 2, we have

$$
\begin{aligned}
& ENT_N(F) \\
=& log(N(F)) - \frac{1}{N(F)} \sum_{st\in E(F)} \sqrt{d_F(s)+d_F(t)} \times log(\sqrt{d_F(s)+d_F(t)}) \\
=& log(N(F)) - \frac{1}{N(F)} \left[\sum_{i=1}^{5} \sum_{st\in E_i(F)} \sqrt{d_F(s)+d_F(t)} \times log(\sqrt{d_F(s)+d_F(t)})\right] \\
=& log(N(F)) - \frac{1}{N(F)} \begin{bmatrix} 4\sqrt{6}\cdot log(\sqrt{6}) + 4\sqrt{8}\cdot log(\sqrt{8}) \\ +(4k+8l)\cdot\sqrt{8}\cdot log(\sqrt{8}) \end{bmatrix} \\
& - \frac{1}{N(F)} \begin{bmatrix} (24k+32l-36)\cdot\sqrt{10}\cdot log(\sqrt{10}) \\ +(60kl-36k-52l+28)\cdot\sqrt{12}\cdot log(\sqrt{12}) \end{bmatrix}.
\end{aligned}
$$

The value of $N(F)$ in the previous expression is substituted to obtain the desired formulation of the Nirmala entropy for $D(Si_2C_3$-$I[k,l])$.

First inverse Nirmala entropy of $D(Si_2C_3$-$I[k,l])$:
From Theorem 2, the first inverse Nirmala index F is given by

$$IN_1(F) = \left(2\sqrt{3} + \frac{8}{\sqrt{6}} + \frac{28}{\sqrt{3}} - 36\sqrt{\frac{10}{24}}\right) + k\left(\frac{4}{\sqrt{2}} + 24\sqrt{\frac{10}{24}} - \frac{36}{\sqrt{3}}\right) + l\left(\frac{8}{\sqrt{2}} + 32\sqrt{\frac{10}{24}} - \frac{52}{\sqrt{3}}\right) + 60\left(\frac{kl}{\sqrt{3}}\right).$$

From (6) and Table 2, we have

$$\begin{aligned}
&ENT_{IN_1}(F)\\
=&log(IN_1(F)) - \frac{1}{IN_1(F)} \sum_{st\in E(F)} \sqrt{\frac{1}{d_F(s)} + \frac{1}{d_F(t)}} \times log\left(\sqrt{\frac{1}{d_F(s)} + \frac{1}{d_F(t)}}\right)\\
=&log(IN_1(F))\\
&- \frac{1}{IN_1(F)} \left[\sum_{i=1}^{5} \sum_{st\in E_i(F)} \sqrt{\frac{1}{d_F(s)} + \frac{1}{d_F(t)}} \times log\left(\sqrt{\frac{1}{d_F(s)} + \frac{1}{d_F(t)}}\right)\right]\\
=&log(IN_1(F)) - \frac{1}{IN_1(F)} \left[2\cdot\sqrt{3}\cdot log\left(\frac{\sqrt{3}}{2}\right) + \frac{8}{\sqrt{6}}\cdot log\left(\frac{2}{\sqrt{6}}\right)\right]\\
&- \frac{1}{IN_1(F)} \left[\frac{(4k+8l)}{\sqrt{2}}\cdot log\left(\frac{1}{\sqrt{2}}\right) + (24k+32l-36)\sqrt{\frac{10}{24}} + log\left(\sqrt{\frac{10}{24}}\right)\right]\\
&- \frac{1}{IN_1(F)} \left[\frac{(60kl-36k-52l+28)}{\sqrt{3}}\cdot log\left(\frac{1}{\sqrt{3}}\right)\right].
\end{aligned}$$

On substituting the value of $IN_1(F)$ into the previous equation, we get the desired expression for the first inverse Nirmala entropy of $D(Si_2C_3$-$I[k,l])$.

Second inverse Nirmala entropy of $D(Si_2C_3$-$I[k,l])$:
The second inverse Nirmala index F is given by

$$IN_2(F) = \left(8\sqrt{3} + 2\sqrt{6} + 28\sqrt{3} - 36\sqrt{\frac{24}{10}}\right) + k\left(4\sqrt{2} + 24\sqrt{\frac{24}{10}} - 36\sqrt{3}\right) + l\left(8\sqrt{2} + 32\sqrt{\frac{24}{10}} - 52\sqrt{3}\right) + 60\left(kl\sqrt{3}\right).$$

From (7) and Table 2, we have

$$
\begin{aligned}
&ENT_{IN_2}(F)\\
=&log(IN_2(F)) - \frac{1}{IN_2(F)} \sum_{st\in E(F)} \frac{\sqrt{d_F(s)\cdot d_F(t)}}{\sqrt{d_F(s)+d_F(t)}} \times log\left(\frac{\sqrt{d_F(s)\cdot d_F(t)}}{\sqrt{d_F(s)+d_F(t)}}\right)\\
=&log(IN_2(F))\\
&- \frac{1}{IN_2(F)} \left[\sum_{i=1}^{5} \sum_{st\in E_i(F)} \frac{\sqrt{d_F(s)\cdot d_F(t)}}{\sqrt{d_F(s)+d_F(t)}} \times log\left(\frac{\sqrt{d_F(s)\cdot d_F(t)}}{\sqrt{d_F(s)+d_F(t)}}\right)\right]\\
=&log(IN_2(F)) - \frac{1}{IN_2(F)} \left[4\sqrt{\frac{8}{6}}\cdot log\left(\sqrt{\frac{8}{6}}\right) + 4\sqrt{\frac{3}{2}}\cdot log\left(\sqrt{\frac{3}{2}}\right)\right]\\
&- \frac{1}{IN_2(F)} \left[(4k+8l)\cdot\sqrt{2}\cdot log\left(\sqrt{2}\right) + (24k+32l-36)\sqrt{\frac{24}{10}} + log\left(\sqrt{\frac{24}{10}}\right)\right]\\
&- \frac{1}{IN_2(F)} \left[(60kl-36k-52l+28)\cdot\sqrt{3}\cdot log\left(\sqrt{3}\right)\right].
\end{aligned}
$$

By adding the value of $IN_2(F)$ to the previous expression, the second inverse Nirmala entropy for $D(Si_2C_3\text{-}I[k,l])$ can be found.

4 Comparison Through Numerical and Graphical Demonstrations

Numerous scientific disciplines, including computer science, information theory, chemistry, and pharmaceutical sciences particularly the study of biological drugs use graph entropy metrics. Thus, the numerical assessment and graphical representation of these molecular descriptors are vital for researchers in these fields. This section presents a comparative analysis of the Nirmala indices and their related entropy measures through numerical computations, surface representations, and three-dimensional line plots. Table 3 shows the numerical results of the Nirmala indices and their associated entropy measures for $D(Si_2C_3\text{-}I[k,l])$ for the range $1 \leq k,l \leq 30$, with the condition that $k = l$.

[k,l]	N	IN_1	IN_2	ENT_N	ENT_{IN_1}	ENT_{IN_2}
[1,1]	118.298346	28.1253138	57.47221116	3.586317328	3.78797439	3.684136134
[2,2]	648.0243692	125.8746645	320.5462752	5.837264747	5.340351376	5.294307092
[3,3]	1593.44259	292.9060475	791.4664361	6.916918089	6.20054332	6.170960783
[4,4]	2954.553	529.2194628	1470.232694	7.623525826	6.7995575	6.777760819
[5,5]	4731.3556	834.8149104	2356.845049	8.147615095	7.25973818	7.242481404
[6,6]	6923.8504	1209.69239	3451.3035	8.563744349	7.63352394	7.619241317
[7,7]	9532.03739	1653.851903	4753.608049	8.908637836	7.94829824	7.936115073
[8,8]	12555.9166	2167.293447	6263.758694	9.203045525	8.2201847	8.20956276
[9,9]	15995.488	2750.017024	7981.755437	9.459821615	8.45948432	8.450068861
[10,10]	19850.7515	3402.022633	9907.598276	9.687474229	8.67318081	8.664725678
[11,11]	24121.7073	4123.310274	12041.28721	9.891923748	8.86622816	8.858555567
[12,12]	28808.3553	4913.879948	14382.82225	10.07745441	9.04226829	9.035245641
[13,13]	33910.6954	5773.731654	16932.20338	10.24726569	9.2040571	9.197582871
[14,14]	39428.7278	6702.865393	19689.4306	10.40380965	9.35373046	9.3477252
[15,15]	45362.4523	7701.281163	22654.50393	10.54900673	9.49297735	9.487377692
[16,16]	51711.869	8768.978966	25827.42335	10.68438892	9.6231564	9.617911025
[17,17]	58476.978	9905.958801	29208.18886	10.81119783	9.74537685	9.740443596
[18,18]	65657.7791	11112.22067	32796.80048	10.93045369	9.86055607	9.855899876
[19,19]	73254.2724	12387.76457	36593.25819	11.04300495	9.96946141	9.965052807
[20,20]	81266.4579	13732.5905	40597.562	11.14956482	10.0727412	10.06855521
[21,21]	89694.3356	15146.69847	44809.7119	11.2507385	10.1709483	10.16696346
[22,22]	98537.9055	16630.08846	49229.70791	11.34704396	10.2645577	10.2607556
[23,23]	107797.168	18182.76049	53857.55	11.43892793	10.3539807	10.35034537
[24,24]	117472.122	19804.71455	58693.2382	11.52677836	10.4395759	10.43609327
[25,25]	127562.768	21495.95065	63736.77249	11.61093431	10.5216576	10.51831532
[26,26]	138069.107	23256.46877	68988.15288	11.69169386	10.6005028	10.59729006
[27,27]	148991.138	25086.26893	74447.37937	11.76932038	10.6763572	10.67326429
[28,28]	160328.861	26985.35112	80114.45195	11.84404781	10.7494394	10.74645769
[29,29]	172082.276	28953.71534	85989.37063	11.91608479	10.8199449	10.81706668
[30,30]	184251.384	30991.3616	92072.13541	11.98561828	10.8880492	10.88526755

Table 3: Calculated values of the Nirmala indices and their associated entropy values of $D(Si_2C_3\text{-}I[k,l])$, where $1 \leq k,l \leq 30$ with $k = l$.

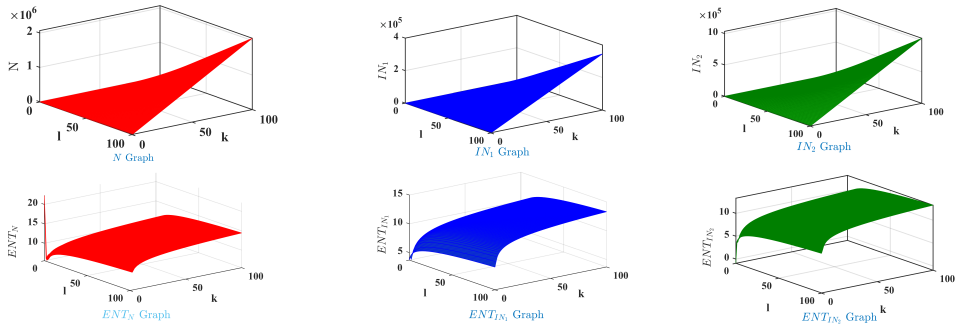

Figure 3: Graphical representation of Nirmala indices and the corresponding entropy measures of $D(Si_2C_3\text{-}I[k,l])$ for the range $1 \leq k,l \leq 100$ with $k = l$.

The surface plots depicting the molecular descriptors being analyzed are illustrated in Figure 3 for $1 \leq k,l \leq 100$ with $k = l$. Furthermore, Figures 4 and 5 present a comparison between the Nirmala indices and the relevant entropy measures, using both surface and 3D line plots for the same range. Based on the information provided in Table 3, and from Figures 4 and 5, we are led to the following observations.

Note 1: As the values of k and l increase, the Nirmala indices and related entropy measures of $D(Si_2C_3\text{-}I[k,l])$ increase as well, confirming their direct proportionality.

Note 2: The following inequality relationships apply to $D(Si_2C_3\text{-}I[k,l])$ as shown in Table 3 and Figures 4 and 5:

$$\begin{gathered} IN_1(F) < IN_2(F) < N(F) \text{ for } 1 \leq k,l \leq 30, \\ ENT_{IN_1}(F) < ENT_N(F); ENT_{IN_2}(F) < ENT_N(F) \text{ for } 2 \leq k,l \leq 30, \\ ENT_{IN_1}(F) \approx ENT_{IN_2}(F) \text{ for } 2 \leq k,l \leq 30. \end{gathered}$$

5 Curve Fitting and Correlation Between Nirmala Indices and Entropy Measures

Curve fitting represents a highly effective and extensively utilized method for data analysis. This technique is employed to examine the relationship

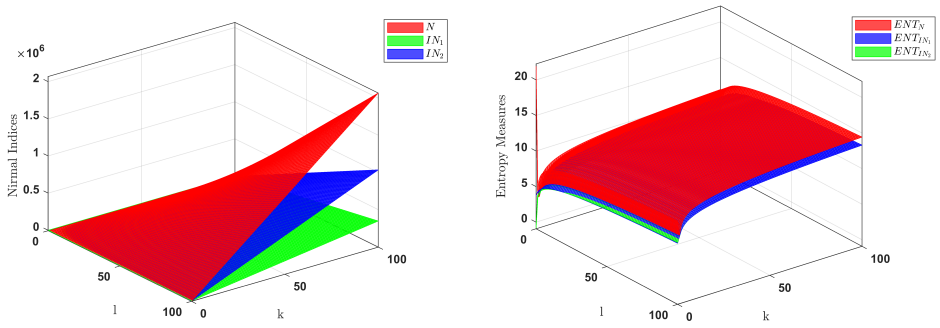

Figure 4: Surface plot.

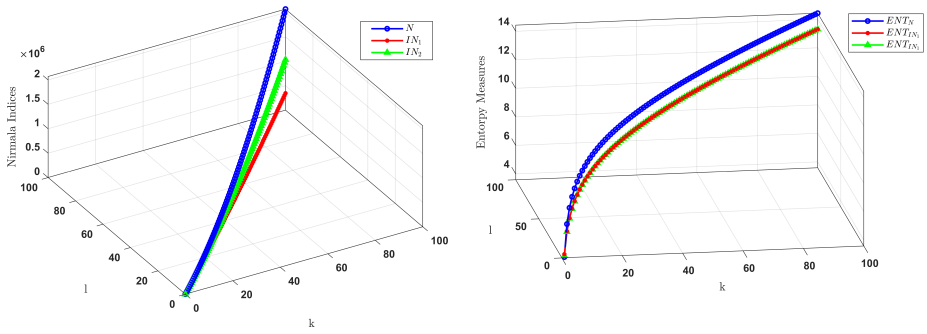

Figure 5: 3D line plot.

between one or more independent variables and a dependent variable, aiming to establish an optimal model that best represents this relationship. Various approaches to curve fitting include polynomial, linear, rational, and power methods. In this study, we conduct a curve fitting analysis to explore the relationship between the Nirmala indices and the entropy measures of $D(Si_2C_3\text{-}I[k,l])$ for the range $1 \leq k,l \leq 100$ with the condition that $k = l$.

The analysis is carried out using a power-2 regression model.

a) General model power-2:

$$ENT_N = \beta_1.N^{\alpha} + \Gamma_1,$$

where coefficients(with 95% confidence bounds(CB) are $\beta_1 = -43.48$ with CB $(-45.67, -41.29)$, $\alpha = -0.03492$ CB $(-0.03757, -0.03227)$ and $\Gamma_1 = 40.47$ with CB $(38.12, 42.81)$.

b) General model power-2:

$$ENT_{IN_1} = \beta_2 . IN_1^{\alpha_1} + \Gamma_2,$$

where coefficients(with 95% confidence bounds(CB) are $\beta_2 = -390.5$ with CB $(-426.6, -354.4)$, $\alpha_1 = -0.002636$ CB $(-0.002886, -0.002386)$ and $\Gamma_2 = 390.9$ with CB $(354.8, 427)$.

c) General model power-2:

$$ENT_{IN_2} = \beta_3 . IN_2^{\alpha_2} + \Gamma_3,$$

where coefficients(with 95% confidence bounds(CB) are $\beta_3 = -204.1$ with CB $(182.8, 225.4)$, $\alpha_2 = 0.004634$ CB $(0.004173, 0.005095)$ and $\Gamma_3 = -204.3$ with CB $(-225.6, -183)$.

The analysis incorporates several statistical measures, including the squared correlation coefficient (R^2), the sum of squared errors (SSE), and the root mean squared error (RMSE). A model is considered to be effective when the RMSE value is low (approaching 0), while a higher R^2 value (approaching 1) indicates a better fit of the regression line to the data. In this study, our primary objective is to achieve a low RMSE. The curve fitting tool in MATLAB is employed to develop the regression models. The statistics derived from these fits are presented in Table 4, and the resulting models are illustrated in Figure 6.

Topological indices	**Data**	**Fit-type**	$\mathbf{R^2}$	**SSE**	**RMSE**
N	N vs. ENT_N	Power-2	1	0.0686	0.00266
IN_1	IN_1 vs. ENT_{IN_1}	Power-2	1	0.0010	0.0032
IN_2	IN_2 vs. ENT_{IN_2}	Power-2	1	0.0037	0.0062

Table 4: Statistics of curve fitting of the Nirmala indices vs. Nirmala entropy measures of $D(Si_2C_3 - I[k, l])$ for the range $1 \leq k, l \leq 100$ with $k = l$.

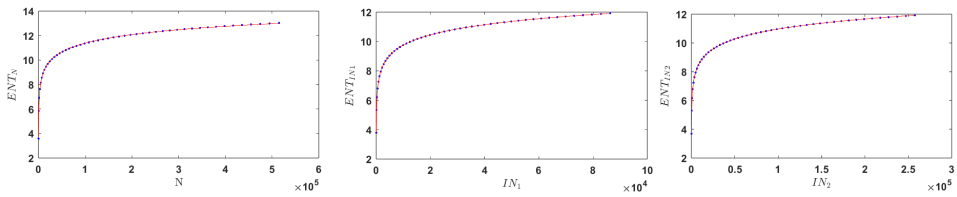

Figure 6: Curve fitting plots for the Nirmala indices vs. associated entropy measures of $D(Si_2C_3\text{-}I[k,l])$ for $1 \leq k,l \leq 100$ with $k = l$.

Correlation analysis is a widely used and effective statistical tool for identifying relationships between two or more data sets. In this study, correlation analysis is applied to investigate the relationship between the Nirmala indices and the associated entropy measures of $D(Si_2C_3\text{-}I[k,l])$, where $1 \leq k,l \leq 100$ with $k = l$. The correlation coefficient (R), which measures the strength of the relationship, is presented in Table 5. The Nirmala indices, as shown in Table 3, exhibit varying values, yet they demonstrate a high correlation, with $R = 0.9988$, indicating a strong relationship.

This suggests that the indices are highly correlated and will likely predict similar structural properties of the silicon carbide network Si_2C_3-$I[k,l]$. Similarly, the entropy measures based on the Nirmala indices also shows a strong correlation with an R value of 0.9988, leading to the conclusion that these measures are closely related.

Based on this analysis, researchers can confidently proceed with using any one of the Nirmala indices and one associated entropy measure in future studies on Si_2C_3-$I[k,l]$.

	N	IN_1	IN_2	ENT_N	ENT_{IN_1}	ENT_{IN_2}
N	1	1	1	0.7532	0.7733	0.7718
IN_1	1	1	1	0.7536	0.7737	0.7722
IN_2	1	1	1	0.7532	0.7733	0.7718
ENT_N	0.7532	0.7536	0.7532	1	0.9988	0.9990
ENT_{IN_1}	0.7733	0.7737	0.7733	0.9988	1	1
ENT_{IN_2}	0.7718	0.7722	0.7718	0.9990	1	1

Table 5: Correlation among the Nirmala indices and associated entropy measures of $D(Si_2C_3\text{-}I[k,l])$ for $1 \leq k,l \leq 100$ with $k = l$.

6 Pearson Correlation Coefficient

The Pearson correlation coefficient, often represented by r, is a statistical measure used to evaluate the strength and direction of the linear relationship between two continuous variables. When $r = 1$ indicates a perfect positive correlation, $r = -1$ signifies a perfect negative correlation and $r = 0$ represents the absence of a linear relationship, the Pearson correlation coefficient ranges from -1 to 1. The Pearson correlation coefficient (r) is given by

$$r = \frac{\sum(X_i - \overline{X})(Y_i - \overline{Y})}{\sqrt{\sum(X_i - \overline{X})^2 \sum(Y_i - \overline{Y})^2}}$$

Here, X_i and Y_i represent individual data points, while X and Y are the means of the respective variables. The summations are taken over all data points. The numerator of the formula calculates the covariance between the two variables, and the denominator normalizes this value by the product of their standard deviations, resulting in a value between -1 and 1.

In this context, the Pearson correlation coefficient is used to determine whether and how indices and entropy are related when they are correlated. A high positive r value would indicate that entropy increases as the index value increases, and vice-versa. Conversely, a large negative r value suggests a tendency for one variable to decrease as the other increases.

To better understand the strength and direction of the relationships between entropy and various Nirmala-based indices, we generated a heatmap using the Pearson correlation coefficient, as illustrated in Figure 7. By examining this heatmap, which visually represents the correlation coefficients, we can identify whether these variables exhibit a positive or negative relationship. This information is essential for understanding the complex interactions between entropy and the indices, as it highlights how variations in entropy might correspond to changes in the index. Consequently, this insight enhances our ability to analyze complex systems and make more informed decisions. However, further research is often necessary to uncover the underlying mechanisms behind these observed relationships.

Our calculations revealed significant correlations between entropy measurements and topological indices, highlighting the connection between the structural properties and complexity of Si_2C_3-$I[k, l]$. These relationships provide valuable insights into the material's potential applications as a conductor for nanoelectronic devices. By employing the Pearson correlation coefficient, we quantified the relationship between the material's entropic

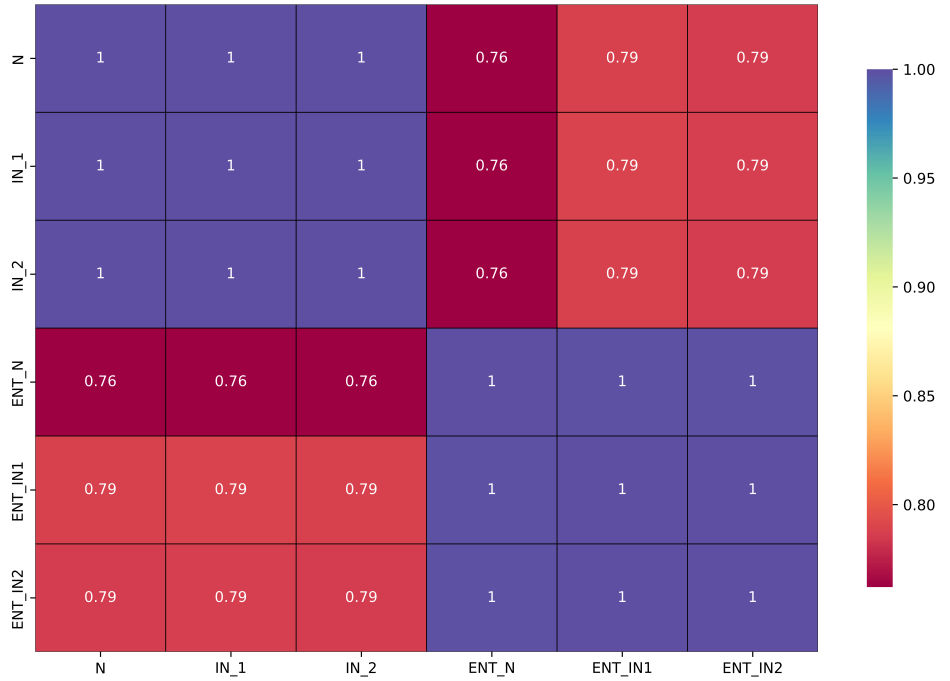

Figure 7: Pearson correlation between indices and entropies of $D(Si_2C_3\text{-}I[k,l])$ for $1 \leq k,l \leq 100$ with $k = l$.

and topological properties, enhancing our understanding of its suitability for advanced technological applications.

7 Applications to HOMO-LUMO Gap and Graph Energy

Based on the notion that the two are approximately proportional, graph energy was introduced as a mathematical abstraction of $\pi-$electron energy. The investigation of molecular orbital theory in conjugated hydrocarbons, including benzene, led to this discovery. Consequently, graph energy has emerged as a valuable instrument for creating mathematical models that examine the stability and reactivity of molecules [49]. The *graph energy* of a molecular graph G is mathematically defined as the sum of the absolute values of the eigenvalues of the adjacency matrix of G. Let $\lambda_1, \lambda_2, \ldots, \lambda_n$ be

the eigenvalues of G of order n. Then the graph energy E_π of G is defined as $E_\pi(G) = \sum_{i=1}^{n} |\lambda_i|$. Determining the eigenvalues from the characteristic polynomial is the main computing challenge of graph energy calculation, and it gets harder for large and complicated graphs. This difficulty has prompted the creation of mathematical models and algorithms.

We refer to [49] for the following definitions. Let n be the number of vertices of the silicon carbide Si_2C_3-$I[k,l]$. The energy of the highest occupied molecular orbital (HOMO) is $E_{HOMO} = \lambda_{\frac{n}{2}}$ and the energy of the lowest unoccupied molecular orbital (LUMO) is $E_{LUMO} = \lambda_{\frac{n}{2}+1}$. Therefore, HOMO-LUMO gap is $\delta_{HL} = \lambda_{\frac{n}{2}} - \lambda_{\frac{n}{2}+1}$.

The total $\pi-$electron energy is $E_\pi = 2\sum_{i=1}^{\frac{n}{2}} \lambda_i$ and the delocalization energy is $E_{Dloc} = E_\pi - n$ [36]. In these formulae, the energies are stated in conventional β-units in Table 6.

Structures	HOMO-LUMO	$\pi-$electron energy/bond	Delocalization energy/bond
$Si_2C_3 - I[1,1]$	0.569613β	1.2451β	0.2451β
$Si_2C_3 - I[2,2]$	0.210617β	1.3964β	0.3964β
$Si_2C_3 - I[3,3]$	0.085688β	1.4452β	0.4452β

Table 6: Energetic properties of Si_2C_3-$I[k,l]$.

As the values of k and l grow, the HOMO-LUMO gaps, which are a sign of kinetic stability, tend to diminish in the Si_2C_3-$I[k,l]$, as seen in Table 6. As k and l are increased, the gap approaches zero (or equals zero). Given this circumstance, the great majority of chains display nearly tiny HOMO-LUMO gaps of Si_2C_3-$I[k,l]$. The energy measurements, which account for both the delocalization energies for each bond and the overall energy of the $\pi-$electron, are shown in Table 6. These observations have been made based on the theoretical estimate of the potential energy.

We now develop a mathematical model for graph energy prediction using Nirmala-based topological indices, as discussed in the earlier section. As shown in Table 7, we calculate the graph energy for particular dimensions

of Si_2C_3-$I[k,l]$ using Python. According to the studies mentioned in [49], we scale the values of the Nirmala indices and the corresponding entropy measures of $D(Si_2C_3$-$I[k,l])$ in Table 2 in accordance with their vertex and edge contributions since the Nirmala indices and the corresponding entropy values increase rapidly with Si_2C_3-$I[k,l]$ structure's dimension. In contrast to the values of the first and second inverse Nirmala indices, our analysis demonstrated that the Nirmala index has a good correlation ($r = 0.89463144$). Therefore, we divide by the number of edges to scale the Nirmala index N. Additionally, as Table 7 illustrates, these scaled index values are then correlated with the graph energy values. Below is the resultant equation.

$$E_\pi(Si_2C_3\textbf{-}I[k,l]) = 10.476567(N^*(Si_2C_3 - I[k,l])) + 0.050070\textbf{, where } N^* = \frac{N}{|E|}.$$

Here, the **correlation coefficient (r):** 0.89463144, F-value (F): 34.55132195, Standard error (SE): 0.18060452.

$[k,l]$	$[1,1]$	$[2,2]$	$[3,3]$
E_π	12.451575	55.856284	130.0678400
N^*	11.82983	12.96049	13.27869

Table 7: Correlation between graph energy and the scaled Nirmala indices (N) of $D(Si_2C_3$-$I[k,l])$.

8 Discussion

Topological indices are numerical values that help describe molecular structures. They are important for studying molecular properties and understanding the behavior of chemical and biological systems. Calculating these indices accurately provides researchers with valuable information about the systems being studied. This work highlights the Nirmala indices, a type of degree-based topological index, applied to the double graph of Si_2C_3-$I[k,l]$.

From Table 3 and Figures 4 and 5, it is evident that the Nirmala indices and their related entropy measures for the double graph of the

silicon carbide network increase as k and l increase. Entropy measures evaluate the uncertainty in a dataset, helping to understand its complexity and distribution. Accurate entropy values offer key insights, improving the understanding of the studied network. This underlines the significance of analyzing the vertex and edge weight entropy for the double graph of Si_2C_3-$I[k,l]$. As shown in Table 3 and Figures 4 and 5, the entropy measures rise with k and l, demonstrating a direct relationship between these variables.

The general power-2 model represents a non-linear regression approach commonly used to analyze non-linear relationships in data, aiding in predictive analysis. Tables 4 and 5 detail the statistical parameters used in this study, including the root mean square error (RMSE), sum of squared errors (SSE), and squared correlation coefficient (R^2). A higher R^2 value, nearing 1, indicates a better fit of the regression line to the data. As shown in Figures 6 and 7 the Nirmala indices and corresponding entropy measures for $D(Si_2C_3$-$I[k,l])$ demonstrate an optimal fit along the curve. The energy properties of several dimensions of Si_2C_3-$I[k,l]$ are shown in Table 6. The graph energy and scaled Nirmala index (N) values of $D(Si_2C_3$-$I[k,l])$ are correlated in Table 7, which also demonstrates that the Nirmala index predicts the graph energy of the silicon carbide network Si_2C_3-$I[k,l]$ with a good correlation ($r = 0.89463144$).

9 Conclusion

In this study, three new graph entropy measures are introduced. These measures are formed using new information functions according to the Nirmala indices' definitions and are called entropy measures based on Nirmala indices. The mathematical formulations of the Nirmala indices for the double graph of silicon carbide network Si_2C_3-$I[k,l]$ have been assessed using its M-polynomial to derive the Nirmala indices-based entropy measures. Additionally, demonstrated the numerical calculations and graphical representations of the Nirmala indices along with their corresponding entropy measures, and conducted a comparative analysis through surface plots. The findings presented in Table 3, and Figures 4 and 5, indicate that the values of the Nirmala indices and the entropy measures of $D(Si_2C_3$-$I[k,l])$ increase with increasing values of k and l, indicating specific relationships among them. We also have the following inequality relationships:

$$IN_1(F) < IN_2(F) < N(F) \text{ for } 1 \leq k,l \leq 30,$$
$$ENT_{IN_1}(F) < ENT_N(F); ENT_{IN_2}(F) < ENT_N(F) \text{ for } 2 \leq k,l \leq 30,$$

$$ENT_{IN_1}(\digamma) \approx ENT_{IN_2}(\digamma) \text{ for } 2 \leq k, l \leq 30.$$

Furthermore, the optimal regression models correlating the Nirmala indices with their corresponding entropies were developed using curve-fitting models. Subsequently, a correlation analysis was conducted among the selected molecular descriptors to evaluate their interrelationships. Lastly, scaled Nirmala index values were used to predict the silicon carbide network's energy values.

The potential limitations of the work: In this study, although the general model power-2 method and Pearson correlation coefficient provided significant insights into the relationship between Nirmala indices and their corresponding entropy measures, there are some limitations to consider. Firstly, our analysis was restricted to the double graph structure of the silicon carbide network, which may limit the applicability of our findings to other network topologies. Future research could expand this methodology to a wider range of graph types and chemical networks to assess the validity of Nirmala-based entropy measures. Moreover, while the general model power-2 method successfully captured the non-linear relationship between the indices and entropy measures, exploring other regression models may provide even more accurate correlations. Furthermore, we focused primarily on Pearson correlation for evaluating the linear relationships; however, exploring other statistical measures or non-linear correlation techniques could offer further insights into complex data patterns.

Future research could also consider the impact of variations in network parameters, such as changes in vertex or edge weights, to investigate their effects on entropy measures. Expanding the study in these directions would provide a deeper understanding of the entropy behavior in various graph-based systems and contribute to refining predictive models for topological indices.

The knowledge gathered from this study is expected to make a substantial contribution to the fields of electronic, optical, and nanoelectronic technologies, especially when it comes to investigating the topology and structural characteristics of the silicon carbide network Si_2C_3-$I[k,l]$.

Funding

No funding is available for this study.

Author contributions

Vijaya Chandra Kumar U and Nagesh H.M: Conceptualization, methodology, and writing - original draft; Madhusudana Reddy M. B: Formal analysis, validation, and visualization.

Declarations

Ethical Approval Not applicable.

Conflict of interests The authors declare that they have no known competing financial interests or personal relationships that could have appeared to influence the work reported in this paper.

References

[1] Deepa Balasubramaniyan, Natarajan Chidambaram, Vignesh Ravi, and Muhammad Kamran Siddiqui. QSPR analysis of anti-asthmatic drugs using some new distance-based topological indices: A comparative study. *International Journal of Quantum Chemistry*, 124(9):e27372, 2024. doi:10.1002/qua.27372.

[2] Zengqiang Chen, Matthias Dehmer, and Yongtang Shi. A note on distance-based graph entropies. *Entropy*, 16(10):5416–5427, 2014. doi:10.3390/e16105416.

[3] Shibsankar Das and Virendra Kumar. Investigation of closed derivation formulas for GQ and QG indices of a graph via M-polynomial. *Iranian Journal of Mathematical Chemistry*, 13(2):129–144, 2022. doi:10.22052/ijmc.2022.246172.1614.

[4] Shibsankar Das and Virendra Kumar. On M-polynomial of the two-dimensional silicon-carbons. *Palestine Journal of Mathematics*, 11:136–157, 2022.

[5] Shibsankar Das and Virendra Kumar. Neighborhood degree sum-based molecular indices and their comparative analysis of some silicon carbide networks. *Physica Scripta*, 99:055941, 2024. doi:10.1088/1402-4896/ad3682.

[6] Shibsankar Das, Virendra Kumar, and Jayjit Barman. Geometric-quadratic and quadratic-geometric indices-based entropy measures of silicon carbide networks. *Silicon*, 17:75–91, 2025. doi:10.1007/s12633-024-03173-8.

[7] Shibsankar Das and Shikha Rai. M-polynomial and related degree-based topological indices of the third type of chain Hex-derived network. *Malaya Journal of Matematik*, 8:1842–1850, 2020. doi:10.26637/MJM0804/0085.

[8] Shibsankar Das and Shikha Rai. M-polynomial and related degree-based topological indices of the third type of Hex-derived network. *Nanosystems Physics Chemistry Mathematics*, 11:267–274, 2020. doi:10.17586/2220-8054-2020-11-3-267-274.

[9] Shibsankar Das and Shikha Rai. On closed derivation formulas of the Nirmala indices from the M-polynomial of a graph. *Journal of the Indian Chemical Society*, 100(6):101017, 2023. doi:10.1016/j.jics.2023.101017.

[10] Hanyuan Deng, Jianguang Yang, and Fangli Xia. A general modeling of some vertex-degree based topological indices in benzenoid systems and phenylenes. *Computers & Mathematics with Applications*, 61(10):3017–3023, 2011. doi:10.1016/j.camwa.2011.03.089.

[11] Emeric Deutsch and Sandi Klavžar. M-polynomial and degree-based topological indices. *Iranian Journal of Mathematical Chemistry*, 6(2):93–102, 2015. doi:10.22052/ijmc.2015.10106.

[12] Boris Furtula and Mert Öz. On properties of the first inverse Nirmala index. *Journal of Mathematical Chemistry*, 63:96–104, 2024. doi:10.1007/s10910-024-01665-x.

[13] Ivan Gutman. Degree-based topological indices. *Croatica Chemica Acta*, 86:351–361, 2013. doi:10.5562/cca2294.

[14] Ivan Gutman and Nenad Trinajstić. Graph theory and molecular orbitals. Total φ-electron energy of alternant hydrocarbons. *Chemical Physics Letters*, 17(4):535–538, 1972. doi:10.1016/0009-2614(72)85099-1.

[15] Haruo Hosoya. On some counting polynomials in chemistry. *Discrete Applied Mathematics*, 19(1):239–257, 1988. doi:10.1016/0166-218X(88)90017-0.

[16] Rongbing Huang, Muhammad Siddiqui, Shazia Manzoor, Sadia Khalid, and Sultan Alaybani. On physical analysis of topological indices via curve fitting for natural polymer of cellulose network. *The European Physical Journal Plus*, 137, 2022. doi:10.1140/epjp/s13360-022-02629-3.

[17] Faiza Ishfaq and M. Faisal Nadeem. Topological properties of fractals via m-polynomial. *Arabian Journal of Mathematics*, 13:303–317, 2024. doi:10.1007/s40065-024-00466-z.

[18] Abdul Khan, Arooj Zia, Francis Campena, Muhammad Siddiqui, Fairouz Tchier, and Shahid Hussain. Investigations of entropy double & strong double graph of silicon carbide. *Silicon*, 16:1–11, 2024. doi:10.1007/s12633-024-02975-0.

[19] Veerabhadrappa R. Kulli. Nirmala index. *International Journal of Mathematics Trends and Technology*, 67(3):8–12, 2021. doi:10.14445/22315373/IJMTT-V67I3P502.

[20] Veerabhadrappa R. Kulli, Lokesha Veera, and K. Nirupadi. Computation of inverse nirmala indices of certain nanostructures. *International Journal of Mathematical Combinatorics*, 2:33–40, 2021.

[21] Virendra Kumar and Shibsankar Das. On Nirmala indices-based entropy measures of silicon carbide networl. *Iranian Journal of Mathematical Chemistry*, 14(4):271–288, 2023. doi:10.22052/ijmc.2023.252742.1704.

[22] Virendra Kumar and Shibsankar Das. Comparative study between Nirmala and Sombor indices based on their applicability, degeneracy and smoothness. *The European Physical Journal Plus*, 139:995, 2024. doi:10.1140/epjp/s13360-024-05768-x.

[23] Virendra Kumar and Shibsankar Das. On structure sensitivity and chemical applicability of some novel degree-based topological indices. *MATCH Communications in Mathematical and in Computer Chemistry*, 92:165–203, 2024. doi:10.46793/match.92-1.165K.

[24] Hadonahalli Mudalagiraiah Nagesh. QSPR analysis with curvilinear regression modeling and temperature-based topological indices, 2024. arXiv:2404.08650.

[25] Hadonahalli Mudalagiraiah Nagesh. Reverse degree-based topological indices and QSPR analysis of cancer drugs, 2024. arXiv:2403.19686.

[26] Hadonahalli Mudalagiraiah Nagesh. Topological analysis of entropy measure using regression model for terpyridine complex nanosheet, 2024. arXiv:2405.20767.

[27] Hadonahalli Mudalagiraiah Nagesh. Topological analysis of entropy measure using regression models for diamond structure, 2024. arXiv:2405.10328.

[28] Hadonahalli Mudalagiraiah Nagesh. Degree-based hybrid topological indices and entropies of wavy zigzag nanoribbons. *International Journal of Quantum Chemistry*, 125(7):e70028, 2025. doi:10.1002/qua.70028.

[29] Hadonahalli Mudalagiraiah Nagesh. Degree-based topological indices and QSPR analysis of Cytomegalovirus drugs. *International Journal of Mathematics for Industry*, 0(0):2450030, 2025. doi:10.1142/S2661335224500308.

[30] Hadonahalli Mudalagiraiah Nagesh and Muguru Chinnaswamy Mahesh Kumar. On the M-polynomial and degree-based topological indices of Dandelion graph. *International Journal of Mathematical Combinatorics*, 1:39–49, 2024.

[31] Hadonahalli Mudalagiraiah Nagesh, U. Vijaya Chandra Kumar, and Muhammad Kamran Siddiqui. Topological indices and entropy measures in cove-edged graphene nanoribbons using curve-fitting models. *Applied Physics A*, 131, 2024. doi:10.1007/s00339-024-08081-7.

[32] Hadonahalli Mudalagiraiah Nagesh and Muhammad Kamran Siddiqui. On Nirmala indices based entropy measures for the complex structure of ruthenium bipyridine, 2024. arXiv:2405.18441.

[33] Hadonahalli Mudalagiraiah Nagesh, Muhammad Kamran Siddiqui, and Imran Cheema. Topological analysis of entropy measure using regression model for silicon carbide network. *The European Physical Journal Plus*, 139, 2024. doi:10.1140/epjp/s13360-024-05641-x.

[34] Shikha Rai and Shibsankar Das. Comparative analysis of M-polynomial based topological indices between poly Hex-derived networks and its subdivision. *Proyecciones (Antofagasta)*, 43(1):69–102, 2024. doi:10.22199/issn.0717-6279-5843.

[35] Milan Randić. Characterization of molecular branching. *Journal of the American Chemical Society*, 97(23):6609–6615, 1975. doi:10.1021/ja00856a001.

[36] Izudin Redžepović, Boris Furtula, and Ivan Gutman. Relating total π-electron energy of benzenoid hydrocarbons with HOMO and LOMO energies. *MATCH Communications in Mathematical and in Computer Chemistry*, 84:229–237, 2020.

[37] Muhammad Sardar, Muhammad Asad Ali, Faraha Ashraf, and Murat Cancan. On topological indices of double and strong double graph of silicon carbide Si_2C_3-$I[k, l]$. *Eurasian Chemical Communications*, 5(1):37–49, 2023. doi:10.22034/ecc.2023.356160.1519.

[38] Claude Elwood Shannon. A mathematical theory of communication. *The Bell System Technical Journal*, 27(3):379–423, 1948. doi:10.1002/j.1538-7305.1948.tb01338.x.

[39] B. Gautham Shenoy, Vishu Kumar M., Divya Acharya, Hadonahalli Mudalagiraiah Nagesh, and Prasanna Poojary. Statistical analysis of Revan topological indices for drug compounds used in treatment of tuberculosis. *Physica Scripta*, 100, 2025. doi:10.1088/1402-4896/ada120.

[40] Haraloor Channakrishnappa Shilpa, Kamanna Gayathri, Ballenahalli Ningegowda Dharmendra, Hadonahalli Mudalagiraiah Nagesh, and Muhammad Kamran Siddiqui. On Nirmala indices–based entropy measures of silicon carbide network Si_2C_3-$III[\alpha, \beta]$. *Iranian Journal of Mathematical Chemistry*, 2023. doi:10.22052/IJMC.2023.252742.1704.

[41] Haraloor Channakrishnappa Shilpa, Kamanna Gayathri, and Hadonahalli Mudalagiraiah Nagesh. M-polynomial and neighborhood M-polynomial of some concise drug structures: A-315675, Oseltamivir carboxylate, Zanamivir, and BCX-1812. *Letters in Applied NanoBioScience*, 13(2), 2024. doi:10.33263/LIANBS132.075.

[42] Haraloor Channakrishnappa Shilpa, Kamanna Gayathri, Hadonahalli Mudalagiraiah Nagesh, and Nittur Narahari. M-polynomials and degree-based topological indices of Mycielskian of paths and cycles. *Communications in Mathematics and Applications*, 14(4):1375–1383, 2023. doi:10.26713/cma.v14i4.2574.

[43] Haraloor Channakrishnappa Shilpa, Kamanna Gayathri, Hadonahalli Mudalagiraiah Nagesh, and Nittur Narahari. On the M-polynomials and degree-based topological indices of an important class of graphs. *International Journal of Mathematical Combinatorics*, 2:38–50, 2023.

[44] Nenad Trinajstić. *Chemical Graph Theory*. CRC Press, 2nd edition, 2018. doi:10.1201/9781315139111.

[45] Ashish Verma, Sourav Mondal, Nilanjan De, Nilanjan De, and Anita Pal. Topological properties of Bismuth tri-iodide using neighborhood M-polynomial. *International Journal of Mathematics Trends and Technology*, 65(10):83–90, 2019. doi:10.14445/22315373/IJMTT-V65I10P512.

[46] Xing-Long Wang, Muhammad Kamran Siddiqui, Syed Ajaz K. Kirmani, Shazia Manzoor, Sarfraz Ahmad, and Mlamuli Dhlamini. On topological analysis of entropy measures for silicon carbides networks. *Complexity*, 2021(1):4178503, 2021. doi:10.1155/2021/4178503.

[47] Harry Wiener. Structural determination of paraffin boiling points. *Journal of the American Chemical Society*, 69(1):17–20, 1947. doi:10.1021/ja01193a005.

[48] Jun Yang, Muhammad Kamran Siddiqui, Mazhar Hussain, Shazia Manzoor, Nazir Hussain, and Zohaib Saddique and. QSPR analysis of some phenolic compounds present in Moringa Oleifera. *Polycyclic Aromatic Compounds*, 44(6):4197–4214, 2024. doi:10.1080/10406638.2023.2247120.

[49] Xiujun Zhang, S. Prabhu, M. Arulperumjothi, S. Manikanda Prabhu, Micheal Arockiaraj, and V. Manimozhi. Distance based topological characterization, graph energy prediction, and NMR patterns of benzene ring embedded in P-type surface in 2D network. *Scientific Reports*, 14:23766, 2024. doi:10.1038/s41598-024-75193-8.

© Scientific Annals of Computer Science 2025